IOP Conf. Series: Materials Science and Engineering **101** (2015) 012055 doi:10.1088/1757-899X/101/1/012055

Magnetic and structural design of a 15 T Nb_3Sn accelerator dipole model

V V Kashikhin[1], N Andreev, E Barzi, I Novitski and A V Zlobin

Fermi National Accelerator Laboratory, Batavia, Illinois, USA

E-mail: vadim@fnal.gov

Abstract. Hadron Colliders (HC) are the most powerful discovery tools in modern high energy physics. A 100 TeV scale HC with a nominal operation field of at least 15 T is being considered for the post-LHC era. The choice of a 15 T nominal field requires using the Nb_3Sn technology. Practical demonstration of this field level in an accelerator-quality magnet and substantial reduction of the magnet costs are the key conditions for realization of such a machine. FNAL has started the development of a 15 T Nb_3Sn dipole demonstrator for a 100 TeV scale HC. The magnet design is based on 4-layer shell type coils, graded between the inner and outer layers to maximize the performance. The experience gained during the 11-T dipole R&D campaign is applied to different aspects of the magnet design. This paper describes the magnetic and structural designs and parameters of the 15 T Nb_3Sn dipole and the steps towards the demonstration model.

1. Introduction

Hadron Colliders (HC) are the most powerful discovery tools in modern high energy physics. Interest to an HC with the energy above the LHC reach gained further momentum in the strategic plans recently developed in the U.S., Europe and China [1]-[3]. To build a ~100 TeV center of mass energy HC in a ~100 km tunnel, ~15 T dipoles operating at 1.9 K or 4.5 K with 15-20% margin are needed. A nominal operating field up to 15-16 T can be provided by the Nb_3Sn technology. A practical demonstration of this field level in accelerator-quality magnets and a substantial reduction of magnet costs are the key conditions for the realization of such a machine.

The main challenges for 15 T Nb_3Sn magnets include considerably higher Lorentz forces and larger stored energy than in existing accelerator magnets. The stronger forces generate higher stresses in the coil and mechanical structure and, thus, may need stress control to maintain them below the level acceptable for the brittle Nb_3Sn conductor. The large stored energy leads to further complications in the magnet quench protection.

FNAL has started the development of a 15 T Nb_3Sn dipole demonstrator for a 100 TeV scale HC based on the optimized “cos-theta” coil design. As a first step, the existing 11 T dipole, developed for the LHC upgrades [4], will be equipped with two outer layers to achieve the field of 15 T in a 60 mm aperture of an interim model. Then, to increase the field margin, the inner 2-layer coil will be replaced with an optimized graded coil.

Magnetic and structural designs and parameters of the interim and optimized 15 T Nb_3Sn dipole demonstration models are described in this paper.

[1] To whom any correspondence should be addressed.

2. Magnet design and parameters

The main objectives of this magnet are demonstration of the 15 T field level in an aperture suitable for future HC and study of the magnet quench performance and margins, quench protection and field quality. Five 4-layer coil cross-sections were designed using two cables with 15 mm width and different thicknesses listed in table 1. The cables use 1.0 mm and 0.7 mm Nb_3Sn strands with a critical current density J_c(15 T, 4.2 K) = 1500 A/mm^2 and a nominal Cu/SC ratio of 1.13. Similar Nb_3Sn cables have already been developed at FNAL and used in previous dipole models [5], [6].

Table 1. Dimensions of reacted bare cables.

Parameter	Units	Cable 1	Cable 2
Number of strands		28	40
Mid-thickness	mm	1.870	1.319
Width	mm	15.10	15.10
Keystone angle	degree	0.805	0.805

Based on the design studies described in [7], graded coil design with the minimal number of turns was selected for the 15 T dipole demonstrator. To make the maximum use of the available resources and reduce the model fabrication time, the two outermost layers will be first assembled and tested with the 60-mm coils used in the 11 T dipole models [4], and then with the optimized inner coils. The cross-sections of the graded and interim coils designed using ROXIE code are shown in figure 1.

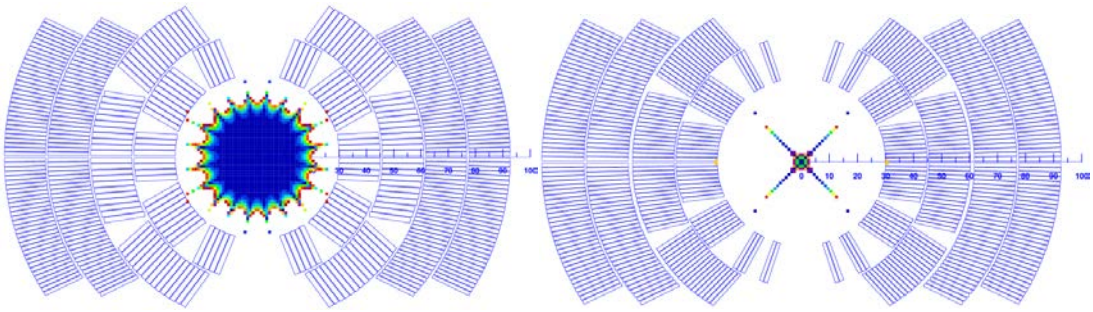

Figure 1. Cross-sections of the graded (left) and the interim (right) coils with the field quality diagram in the coil aperture. The shaded zone represents the field uniformity better than 2×10^{-4}.

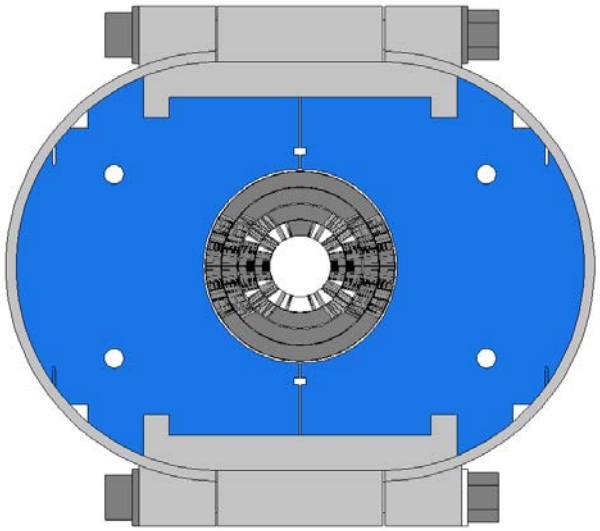

Figure 2. Cold mass cross-section with the “interim” dipole coil.

Cross-section of the 15 T dipole demonstrator cold mass is shown in figure 2. The coils are supported by a vertically split iron yoke, two stainless steel clamps, and a thick stainless steel skin. The cold-mass length is ~1 m long. The maximum cold mass transverse size is ~610 mm, which is limited by the FNAL test cryostat dimensions.

The coil assembly, surrounded by a 2 mm stainless steel spacer, is placed in between two half-yokes braced with two clamps. The bolted skin and the clamps are pre-tensioned under the press to provide an initial coil pre-stress at room temperature. Two thick end plates bolted to the outer shell restrict the longitudinal coil motion under the axial Lorentz forces. Quench protection heaters composed of stainless steel strips are placed between the 2nd and 3rd coil layers and on the coil outer layer.

The calculated 2D design parameters of the 15 T dipole demonstrator are reported in table 2, and the field distribution in the coil and yoke is shown in figure 3. In the interim design with the 11 T dipole coils, the maximum bore field at 4.2 K is 14.6 T, whereas in the optimal graded design it reaches 15.6 T. Reducing the temperature to 1.9 K allows increasing the maximum bore field by ~10% with respect to the values shown in table 2.

Table 2. Magnet design parameters at 4.2 K.

Parameter	Units	Interim	Graded
Bore field at short sample limit	T	14.61	15.59
Peak field at short sample limit	T	15.12	16.23
Current at short sample limit, I_c	kA	9.07	11.40
Inductance at I_c	mH/m	31.86	25.37
Stored energy at I_c	MJ/m	1.31	1.65
Horizontal Lorentz force per quadrant at I_c	MN/m	6.01	7.28
Vertical Lorentz force per quadrant at I_c	MN/m	-3.70	-4.52

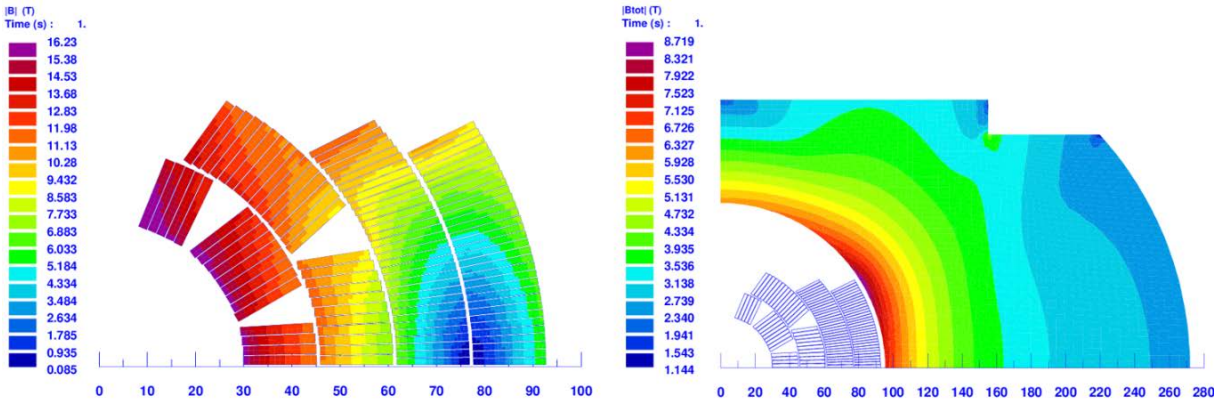

Figure 3. 2D field distribution in the optimal coil (left) and the iron yoke (right).

Geometrical harmonics in the magnet body are summarized in table 3. The optimized coil design shows low geometrical harmonics. In the interim design, there is a large sextupole component because in that case the two outer layers are not optimized to work together with the existing 11-T coil.

Dependences of the magnetic field and the low order harmonics on the current are presented in figure 4. There is a large iron saturation effect in the sextupole component. No special correction is envisioned for the demonstrator that will be used to measure the unaltered weakly-coupled coil magnetization and iron saturation effects, and benchmark the computation codes. For the next models, a persistent current corrector, similar to the one developed for previous magnets [8] will be designed in conjunction with placing holes at appropriate locations within the iron yoke – the techniques also previously applied at FNAL [9] - to suppress both non-linear effects.

Table 3. Field harmonics (in 10^{-4} of the dipole component) in the magnet body at R_{ref}=17 mm.

Harmonic	Interim	Graded
b_3	93.2575	0.0018
b_5	-0.8684	0.0154
b_7	-0.1433	0.0523
b_9	0.4503	0.0612

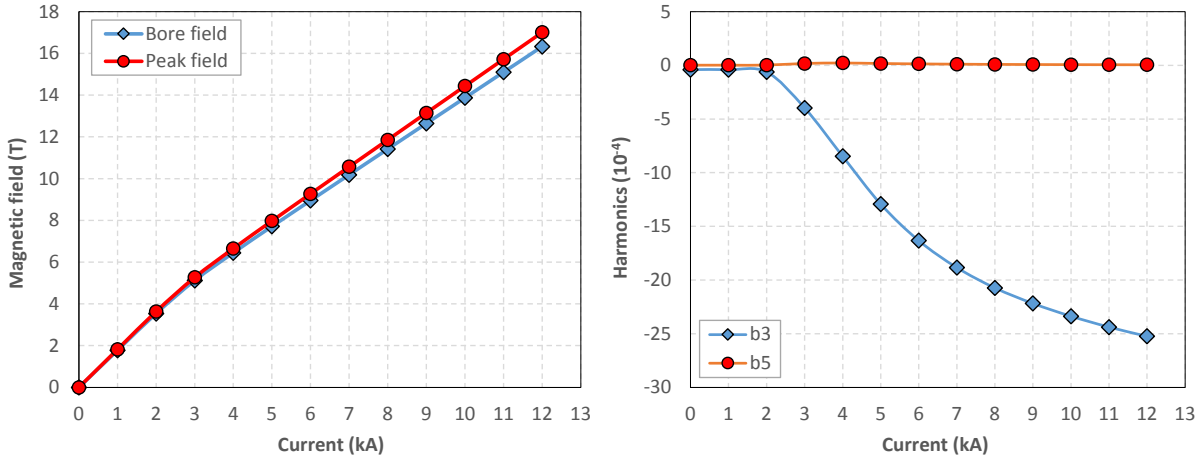

Figure 4. Magnet load lines (left) and low-order harmonics (right) as functions of current.

3. 3D magnetic analysis

The 3D magnetic analysis was performed using Vector Fields OPERA 3D code. Figure 5 shows the coil and yoke designs with the magnetic field distribution. The end length of layers 3 and 4 was minimized in order to increase the length of the straight section. Small end spacers were used in these layers to split the large blocks and reduce the turn inclination build-up. It was preferable to extend the iron yoke over the coil ends for structural reasons. In that case, the peak field point limiting the magnet performance is in the coil end. To reduce the field enhancement in the coil ends with respect to the magnet straight section, the pole blocks of layer 1 and 2 were shifted towards the magnet center.

A cylindrical cut-out was introduced in the ends of the iron yoke, as shown in figure 5 in order to evaluate its effect on reducing the peak field in the ends. Figure 6 shows the ratio between the peak field in the coil and in the central cross-section as a function of the axial coordinate. There is a 2% field enhancement in the coil end without the cutout. Removing 45 mm of the iron material around the coil ends helps to reduce the peak field in the end to the value of the peak field in the central section.

4. Mechanical analysis

Finite element analysis using a parametric 2D ANSYS model has been performed to optimize the stress in the coil and major elements of the magnet support structure, and to minimize the conductor motion and magnet cross-section deformation at room and operation temperatures. The analysis was done for the available 12.7-mm-thick bolted skin, used in several FNAL dipole and quadrupole models, and the 20-mm-thick bolted skin (figure 7). The baseline materials used in the magnet and their properties are listed in table 4. The data for Nb_3Sn coil are based on measurements reported in [10]. Analysis was also performed with Ti and Al bronze poles in coil layers 3 and 4, and Al clamps. The goal of mechanical structure optimization was to maintain the coils under compression up to the ultimate design field of 15 T and the maximum coil stress below ~180 MPa during magnet assembly and operation.

Distributions of the equivalent stress in coils after assembly at room temperature, cool down to the operation temperature of 4.2 K and at the maximum design field of 15 T are shown in figure 8 for both the interim coil with 12.7 mm skin and the graded coil with 20 mm skin. The average transverse stress in the pole and mid-plane turns of the coil layers at the above stages is summarized in table 5.

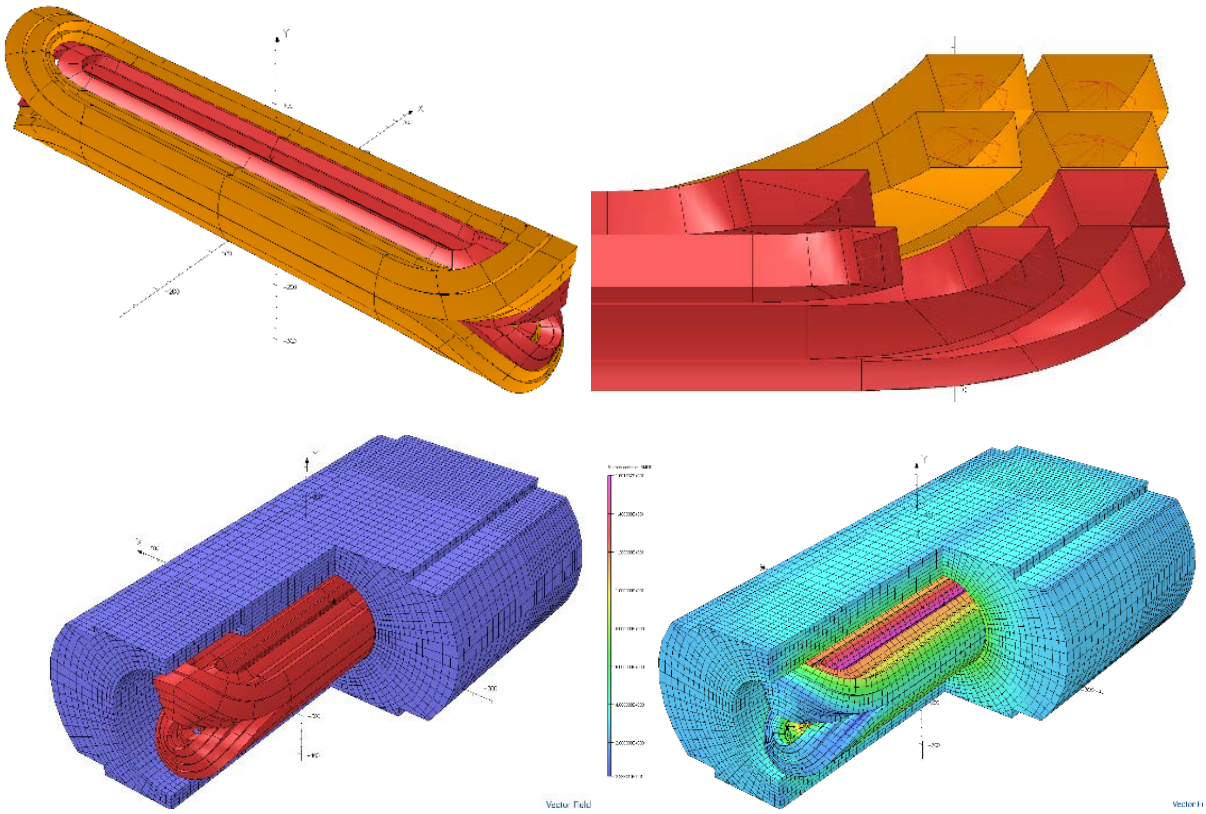

Figure 5. Complete coil (top left), the coil end cross-section (top right), iron yoke design (bottom left) and the field distribution in the coil and yoke (bottom right).

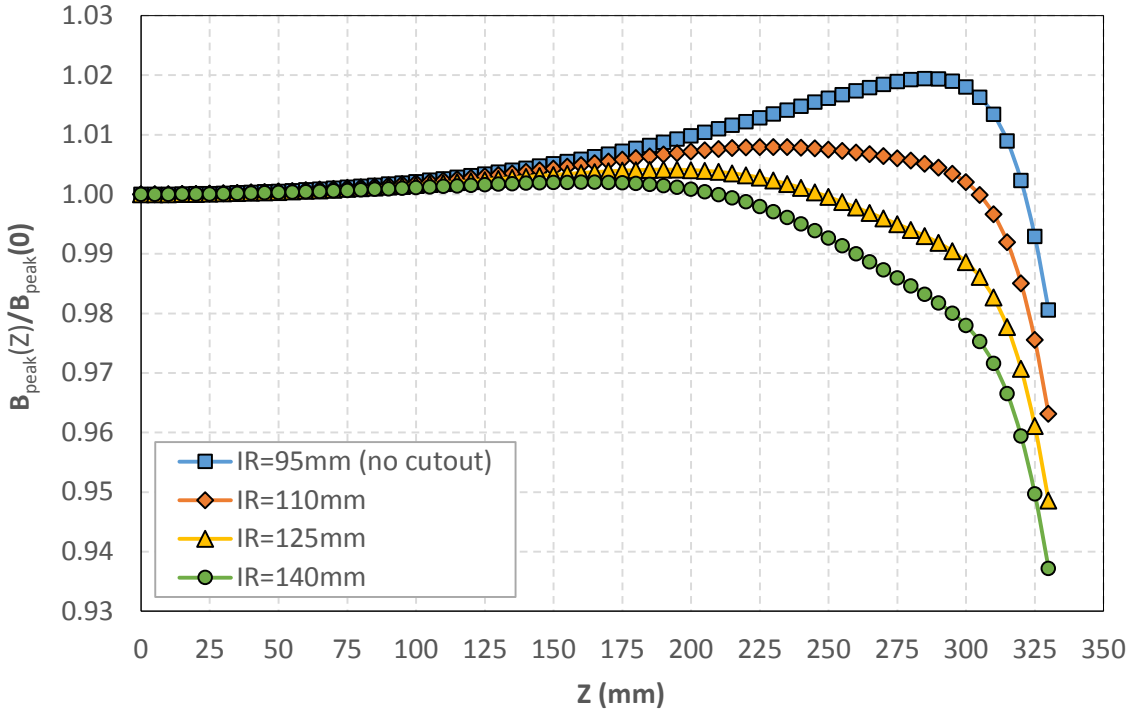

Figure 6. Ratio between the peak field in the coil end and the central section vs. the axial coordinate.

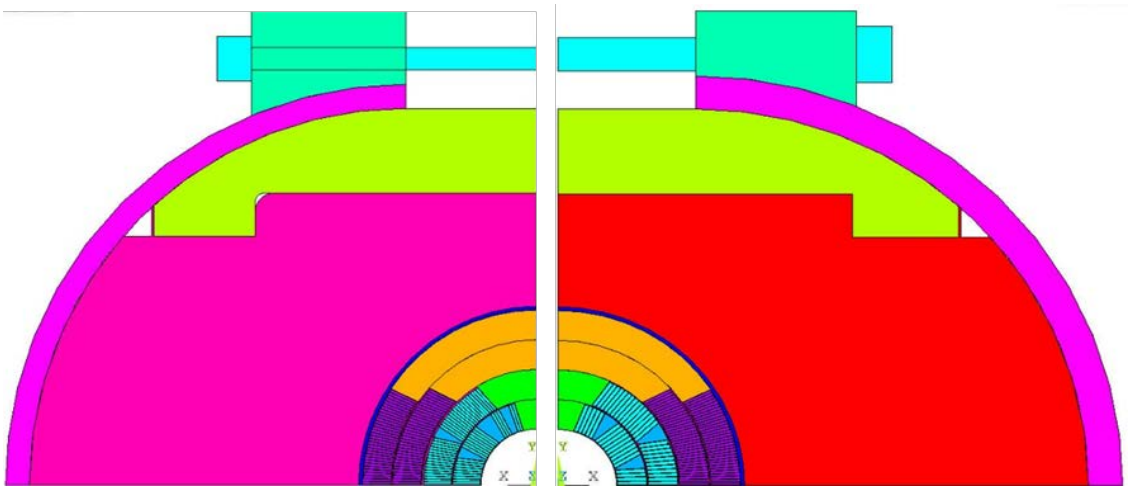

Figure 7. ANSYS model of 15 T dipole demonstrator with interim coil and 12.7 mm bolted skin (left) and graded coil and 20 mm bolted skin (right).

Table 4. Material properties.

Structural element	Material	Thermal contr. (300-2 K), mm/m	Elasticity modulus, GPa		Yield strength, MPa	
			warm	cold	warm	cold
Coil (rad/azim)	Nb_3Sn Composite	2.9/3.3	35/20	40/40	n/a	n/a
Pole blocks	Ti-6Al-4V (layers 1 & 2)	1.7	115	125	650	>900
	Stainless steel (layers 3 & 4)	2.9	195	215	230	500
Wedges	Stainless steel 316	2.9	195	215	230	500
Coil-yoke spacer	Stainless steel 316	2.9	190	210	230	500
Clamp	Stainless steel, grade TBD	2.9	195	215	520	850
Yoke	Iron 1045	2.0	210	225	350	500
Skin	Stainless steel 304L	2.9	190	210	230	500
Bolt	Stainless steel, grade TBD	2.9	195	215	520	850

Table 5. Average azimuthal coil stress in pole and midplane turns of interim coil design with 12.7 mm bolted skin and graded coil design with 20 mm bolted skin (MPa).

Position in coil	Assembly		Cool down		B=15 T	
	Interim	Graded	Interim	Graded	Interim	Graded
Pole 1	100	108	110	148	0	2
Pole 2	60	56	75	71	8	17
Pole 3	75	80	82	99	18	27
Pole 4	85	77	97	94	68	55
Mid-plane 1	70	99	70	96	146	155
Mid-plane 2	80	103	100	111	122	122
Mid-plane 3	80	96	88	89	138	146
Mid-plane 4	80	101	94	103	127	144

In both cases, the maximum equivalent coil stress at room temperature is in the inner-layer pole 1 turn on the level of 114-120 MPa. Due to higher rigidity of the 20-mm skin, the maximum equivalent coil stress increases to 158 MPa which allows keeping IL pole turns under compression at up to 15 T bore field (figure 8). The 12.7 mm skin allows keeping the coil under compression at only up to 13 T bore field. At higher fields, a gap between the inner-layer pole 1 turn and the pole 1 block appears reaching 60 microns at 15 T bore field. Three other coil layers are in contact with their pole blocks (table 5). The maximum equivalent coil stress at the bore field of 15 T is close to 180 MPa in the inner layer mid-plane turns which may limits the magnet performance at higher fields.

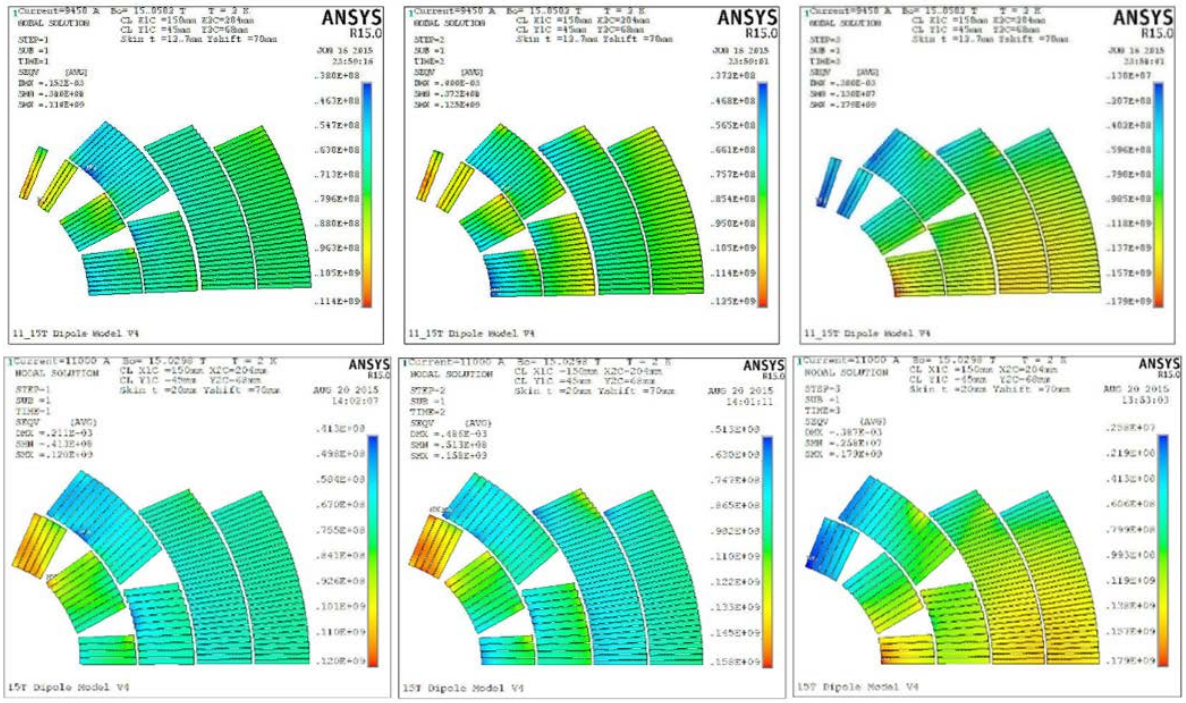

Figure 8. Stress distribution in the interim coil with 12.7 mm skin (top row) and graded coil with 20 mm skin (bottom row).

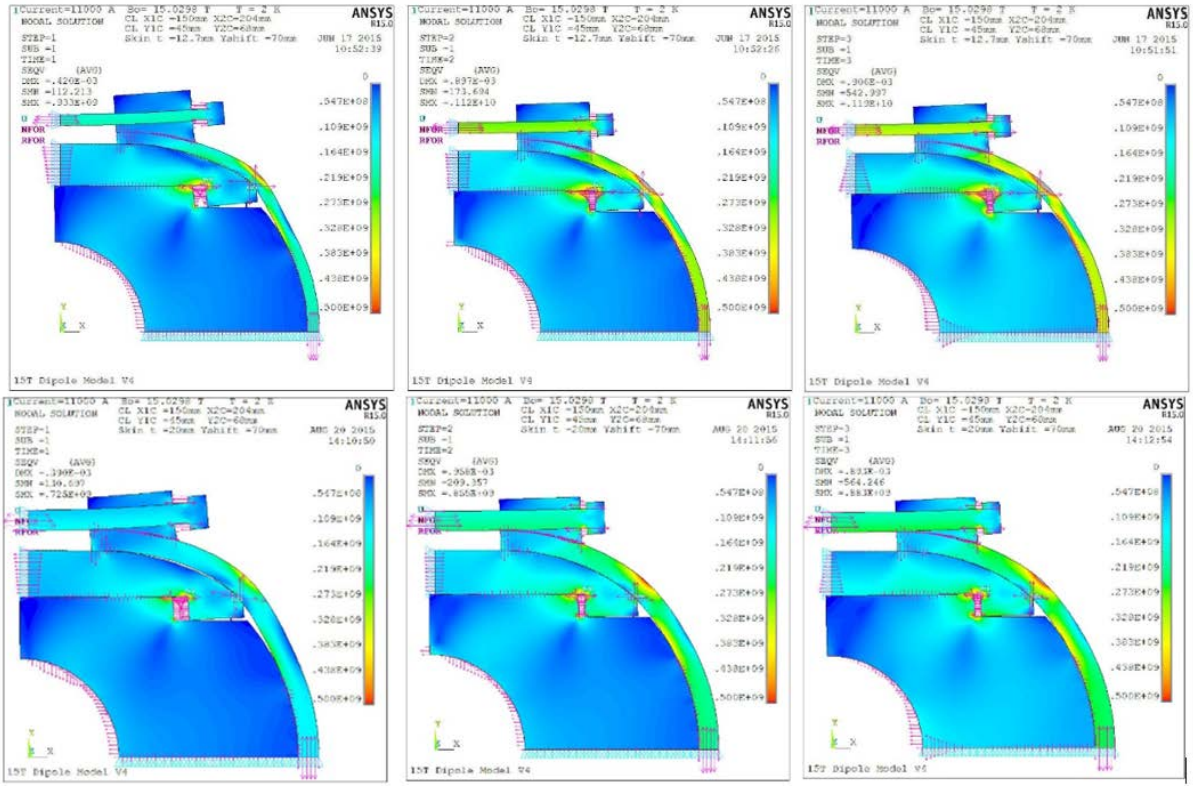

Figure 9. Stress distribution in the dipole mechanical structure with 12.7 mm (top row) and 20 mm (bottom row) skins.

Stress distribution diagrams in the dipole mechanical structure for both the interim coil with 12.7 mm bolted skin and the graded coil with 20 mm bolted skin are shown in figure 9. The maximum stress values in the major elements of the magnet support structure calculated at different assembly and operation stages are presented in table 6. All the numbers are obtained using the model with elastic material properties. Two areas, the yoke-clamp and the skin-clamp interfaces, show rather high local stresses. The high stress concentration on the iron-clamp interface can be reduced to the acceptable level by rounding sharp corners, optimizing the interface contours and using thin spacers made of a softer material. Due to the large stress, the available 12.7-mm skin is not optimal for operation at the design fields up to 15 T. The stress level in the 20-mm skin is acceptable at all temperatures and fields up to 15 T.

Table 6. Maximum stress in structural components (MPa).

Structural element	Interim coil with 12.7 mm bolted skin			Graded coil with 20 mm bolted skin		
	Assembly	Cool down	B=15 T	Assembly	Cool down	B=15 T
Yoke	770	950	810	500	570	760
Clamp	850	1070	1100	725	850	880
Skin aver/max	185/620	300/830	320/880	120/380	210/500	230/550
Bolt	320	500	550	270	450	500

5. Conclusions

Dipole magnets with operating fields of ~15 T are needed for a future HC. An early demonstration of the accelerator quality dipole of this class is a critical milestone to support feasibility of this machine. A 15 T Nb_3Sn dipole demonstrator for a HC based on a 4-layer graded cos-theta coil with 60 mm aperture and cold iron yoke is being developed at FNAL. The magnet design and analysis is in progress with a goal of first model tests in 2016.

Acknowledgment

The work supported by Fermi Research Alliance, LLC, under contract No. DE-AC02-07CH11359 with the U.S. Department of Energy.

References

[1] Building for Discovery: Strategic Plan for U.S. Particle Physics in the Global Context *P5 Report* http://science.energy.gov/~/media/hep/hepap/pdf/May%202014/FINAL_P5_Report_053014.pdf
[2] 2014 *Future Circular Collider Study Kickoff Meeting* Geneva Switzerland http://indico.cern.ch/event/282344/timetable/#20140212
[3] CEPC/SppC study in China http://indico.cern.ch/event/282344/session/1/contribution/65/material/slides/1.pdf
[4] Zlobin A V et al. 2015 11 T Twin-Aperture Nb3Sn Dipole Development for LHC Upgrades *IEEE Trans. on Appl. Supercond.* vol **25** issue 3 4002209
[5] Andreev N et al. 2007 Development of Rutherford-type Cables for High Field Accelerator Magnets at Fermilab *IEEE Trans. on Appl. Supercond*. vol **17** issue 2 p 1027
[6] Barzi E et al. 2012 Development and Fabrication of Nb_3Sn Rutherford Cable for the 11 T DS Dipole Demonstration Model *IEEE Trans. on Appl. Supercond*. vol **22** issue 3 6000805
[7] Zlobin A V et al. 2015 Design concept and parameters of a 15 T Nb_3Sn dipole demonstrator for a 100 TeV hadron collider *Proc. IPAC-2015* Richmond VA USA
[8] Kashikhin V V et al. 2003 Passive Correction of the Persistent Current Effect in Nb_3Sn Accelerator Magnets *IEEE Trans. Appl. Supercond*. vol **13**, no 2, pp 1270-73
[9] Ambrosio G et al. 2000 Magnetic Design of the Fermilab 11 T Nb_3Sn Short Dipole Model *IEEE Trans. Appl. Supercond*. vol **10** no 1 pp 322-25
[10] Chichili D R et al. 2000 Investigation of Cable Insulation and Thermo-Mechanical Properties of Epoxy Impregnated Nb_3Sn Composite *IEEE Trans. on Applied Supercond.*, vol **10** no 1 p 1317